

## 9. CLAY CONDUCTION AND PORE STRUCTURE OF OCEANIC BASALTS FROM DSDP/ODP HOLE 504B<sup>1</sup>

Philippe A. Pezard,<sup>2</sup> James J. Howard,<sup>3</sup> and Michael A. Lovell<sup>4</sup>

### ABSTRACT

The resistivity, porosity, and cation exchange capacity of 36 basaltic samples recovered in Hole 504B during four DSDP and ODP legs have been measured in the laboratory at room temperature and atmospheric pressure. The presence of chlorites and particularly smectites as alteration products of basalt phases is reflected by high values of cation exchange capacity (CEC). Whereas the massive units of Layers 2A and 2B are defined by high and uniform CEC values, the more fractured and altered pillows are characterized in the entire hole by even higher values of CEC and a large variability. The lowest CEC values, measured for the massive units of Layer 2C, are due to changes of basalt alteration facies with depth and the related decreasing abundance of smectites with increasing depth in the oceanic crust.

The porosity and the apparent formation factor (computed from resistivity measurements made with a fluid salinity similar to that of seawater) are related by an inverse power law similar to Archie's formula, with  $m$  close to 1.0 and  $a$  as large as 9.1. A review of the literature shows that such a low  $m$  value equates to current conduction in cracks and microcracks present throughout the rock. The presence of these microstructures reflects the extensional regime under which the rock formed at the ridge axis, and they were conserved by precipitation of clay minerals attributable to intense hydrothermal circulation. The comparison of these results to similar studies of mid-ocean ridge basalt physical properties indicates that  $m$  tends to increase to values close to 2.0 with age. Such values are, in fact, similar to those found for sedimentary rocks and probably reflect an increased tortuosity of the conducting pore space with increasing age. An inverse relationship also relates CEC and apparent formation factor, indicating that surface conduction of clay minerals plays an important role during downhole electrical experiments. This provides a plausible key to the paradox of low permeability and high apparent porosity obtained from comparing the *in-situ* experiments conducted in Hole 504B.

### INTRODUCTION

The study of the physical structure of oceanic plates has been a subject of widespread interest in geosciences over the past 50 yr, particularly since the advent of plate tectonics in the 1960s. Several Deep Sea Drilling Project (DSDP)/Ocean Drilling Program (ODP) drilling campaigns (e.g., Anderson, Honnorez, et al., 1985; Donnelly, Francheteau, et al., 1980), seismic and electromagnetic remote-sensing investigation (Houtz and Ewing, 1976; Luyendyk and Macdonald, 1977; Francheteau, 1983; Cox, 1971; Young and Cox, 1981; Cox et al., 1986), and direct exploration of mid-ocean ridges with submersibles (ARCYANA, 1975; Ballard et al., 1975; Macdonald, 1983) have permitted the construction of an important data base on the upper structure of oceanic plates. The comparison of oceanic heatflow measurements to theoretical cooling plate models (Sclater and Francheteau, 1970; Lister, 1972, 1974; Anderson and Hobart, 1976), and the discovery of "black smokers" (Corliss et al., 1979; Spiess et al., 1980) have demonstrated that the oceanic crust is a porous medium permeated by convecting hydrothermal fluids (Lister, 1972, 1974; Williams et al., 1974). As evolved seawater circulates and reacts with igneous phases of the basaltic crust to produce alteration minerals, it rapidly contributes to the plugging of the existing pore space, partly sealing the crust. In turn, this gradual sealing prevents fluid circulation and reduces the alteration rate of the crust. The oceanic crust consequently operates

as a giant buffer to worldwide ocean water, keeping, for instance, its salinity constant over hundreds of million years by means of this hydrochemical regulation (Sleep and Wolery, 1978; Edmond et al., 1979). Thus, the circulation of seawater in the pore spaces of the crust stands as one of the dominant processes of aging of oceanic plates. Understanding the evolution of this complex filtering process with the description of the porosity and of the permeability structure of the upper crust, therefore, is of prime interest in the context of plate tectonics and the study of the earth as a regulated system.

Unlike bulk density, acoustic velocity, or electrical resistivity, *in-situ* measurements of porosity and permeability of the basaltic crust are not at present directly measurable with geophysical logs. Whereas porosity is estimated routinely from resistivity (Archie, 1942), nuclear (Ellis, 1987), or acoustic experiments in sedimentary formations (Wyllie and Gregory, 1953; Wyllie et al., 1958), the very different structure of the pore space of crystalline rocks or the presence as traces of elements such as gadolinium or boron (with large capture cross-sections to neutrons) has prevented to date the development of an accurate method for deriving porosity from *in-situ* geophysical measurements. Because permeability is not only governed by porosity, but also by the size, shape, tortuosity, and arrangement of the pore space (all of which are difficult to evaluate) and probably other parameters, such as ambient stresses, no precise derivation of permeability has been obtained uniquely from geophysical logs.

In the course of ocean drilling, Anderson and Zoback (1982), Hickman et al. (1984), Anderson, Honnorez, et al. (1985), and Becker, Sakai, et al. (1988) have shown that only measurements of permeability made *in situ* with a hydraulic packer are suitable to study the variations with depth and the modifications with age of this "filtering" system. In Hole 504B, the comparison of these direct permeability measurements with porosity profiles derived from Archie's law using long-spacing measurements of electrical resistivity (Becker, 1985; Becker, Sakai, et al., 1988)

<sup>1</sup> Becker, K., Sakai, H., et al., 1989. *Proc. ODP, Sci. Results*, 111: College Station, TX (Ocean Drilling Program).

<sup>2</sup> Lamont-Doherty Geological Observatory, Palisades, NY 10964, and Department of Geological Sciences, Columbia University, NY 10964.

<sup>3</sup> Schlumberger Doll Research, P.O. Box 307, Old Quarry Road, Ridgefield, CT 06877.

<sup>4</sup> University of Nottingham, Geology Department, Nottingham, NG7 2RD U.K.

has (1) confirmed the vertical zonation of the oceanic crust known from ophiolite studies (Gass and Smewing, 1973; Kidd, 1977; Stern and Elthon, 1979), (2) emphasized the overall decrease in porosity and permeability of the crust with increasing depth, and (3) outlined the limitations of this resistivity-porosity-permeability transform in sections thought to be porous (up to 10% porosity at the base of Layer 2B in Hole 504B) but measured as poorly permeable (on the order of 0.01 mD; Becker, Sakai, et al., 1988).

In this paper, a series of core measurements is reported in order to evaluate whether the presence of clay minerals in the oceanic crust might constitute a significant contribution to current conduction during resistivity logging, which would cause estimates of porosity through Archie's law to be too high. The results are discussed in terms of structure of the pore space, in relation to the porosity-permeability anomaly described previously.

### RESISTIVITY MEASUREMENTS IN HOLE 504B

On ODP Leg 111, the drillship *JOIDES Resolution* returned to Site 504, in the eastern equatorial Pacific. Hole 504B, the deepest borehole drilled yet into the oceanic crust, was reentered to study the crustal structure and the hydrothermal processes at this well-sedimented reference site. The drill hole is located about 200 km to the south of the Costa Rica Rift, in 5.9-m.y.-old oceanic crust. Hole 504B was cored and logged by four DSDP legs (69, 70, 83, and 92) and was deepened 213.3 m into the sheeted dikes of Layer 2C during Leg 111 to a total depth of 1562.3 m below seafloor (mbsf), penetrating 274.5 m of sediments and 1287.8 m of intensely fractured basaltic basement. Leg 111 provided the opportunity to conduct an extensive suite of *in-situ* experiments, including the recording of continuous electrical resistivity over the entire length of the penetrated basement.

The extreme sensitivity of electrical properties to a large number of parameters makes electromagnetic methods both a complex and powerful technique with which to study large- and small-scale structures of rock formations. Although the known electrical properties of rocks and minerals were observed to vary over 24 orders of magnitude in the Earth (Olhoeft, 1981), the measurements made thus far in the oceanic crust have covered less than 6 orders of magnitude. In that respect, *in-situ* measurements of electrical resistivity respond directly to conductivity changes in the rock surrounding the borehole. The presence of vesicular pores, cracks, and microcracks, either filled with fluid or plugged with precipitated conductive alteration minerals such as chlorite and smectite, creates a path for current flow. The electrical conduction is a combination of electrolytic mechanism for the pore space and the fluid-filled fractures and a surface-mediated ion transport mechanism for conductive alteration minerals. Because an order of magnitude separates the resistivity of clays (a few ohm-m *in situ*) from that of seawater (about 0.2 ohm-m at 25°C), the measurements of electrical resistivity are sensitive to the progressive sealing of the oceanic crust with basalt alteration products.

The resistivity of a saturated rock depends not only on the pore space geometry but also on the connectivity of the pores, the distribution of alteration products, and the connectivity of their active surfaces. As a consequence, the difficulty of describing precisely the topology of the pore space and the distribution of alteration products led several authors in the past to use empirical formulae such as Archie's law to relate resistivity and porosity. Such a power law was used in widely differing cases such as clastic sediments (Archie, 1942; Jackson et al., 1978; Lovell, 1985), basalt (Drury and Hyndman, 1979; Kirkpatrick, 1979; Becker, 1985; Broglia and Moos, 1988), or even partly melted crustal rocks by analogy to sedimentary rocks (Waff, 1974; Shankland and Waff, 1977; Hermance, 1979). A similar type of power law was derived in the laboratory from

the study of pressurized samples for a large collection of rocks (Brace et al., 1965; Brace and Orange, 1968a, 1968b).

In order to study how *in-situ* measurements of electrical resistivity are related to both porosity and alteration through possible surface conduction of clays (Drury and Hyndman, 1979; Olhoeft, 1981; Becker, 1985; Karato, 1985), 36 basaltic cores from Hole 504B were sampled at the core repository and then analyzed in the laboratory. This paper focuses on the analysis of the core measurements made at atmospheric pressure and room temperature. The analysis is aimed first at verifying the power law generally accepted as relating resistivity to porosity in basalt (Brace and Orange, 1968a; Drury and Hyndman, 1979; Rai and Manghnani, 1981; Becker, 1985) and, second, at evaluating whether alteration minerals might play a significant role in measurements of electrical resistivity recorded *in situ*. Our results are then compared with previous studies of basalts and granites (Drury and Hyndman, 1979; Kirkpatrick, 1979; Pape et al., 1985; Broglia and Moos, 1988), and a simple model for the evolution of the pore space of the oceanic crust due to hydrothermal alteration is submitted. In a companion manuscript (Pezard and Anderson, this volume), these results are compared with *in-situ* electrical resistivity experiments to analyze their response to structural basement features (such as fault zones, fractures, alteration, or distinct lithologic units), to large-scale layers of the oceanic crust, and, ultimately, to changes with depth of physical properties such as porosity and permeability.

### CORE MEASUREMENTS

Thirty-six basalt minicores were sampled from the DSDP/ODP core repository in order to measure porosity, electrical resistivity, and cation exchange capacity (CEC). Prior to this study, the samples were stored dry and refrigerated for an average period of 4 yr. The samples were first resaturated with distilled water to eliminate the salts deposited in the pore space while drying in storage and subsequently dried for dry weight measurements and then saturated with a 0.195 ohm-m NaCl solution under near-vacuum conditions. During the course of the measurements, the samples were stored in the 0.195 ohm-m NaCl solution (a salinity similar to that of seawater), and the bath was checked regularly for constant salinity.

Most of the samples were selected from the massive units of Layers 2A and 2B (26 out of 36; Table 1). Among the remaining minicores, five represent the fractured pillow units of Layers 2A and 2B, and five the massive units of the upper part of Layer 2C. In addition to these 36 minicores, powders from 29 samples already studied for their alteration content were subjected to electrochemical analysis of CEC (Table 1). Five of these 29 samples come from massive units of Layer 2B, 12 from pillow units of Layer 2B, and the remaining 12 from various units of Layer 2C and the transition zone (Anderson, Honnorez, et al., 1985). A total of 65 samples from Hole 504B was analyzed in this study.

#### Cation Exchange Capacity Measurements

The measurement of CEC is commonly used to evaluate the shaliness of a sedimentary formation in the context of the oil industry. The objective of this electrochemical analysis is to count the number of free cations that might contribute to the conduction of current during an electromagnetic experiment. Smectites, and to a lesser extent chlorites, were often observed as alteration products of basalt phases in Hole 504B (Alt and Emmermann, 1985; Alt et al., 1985, 1986; Adamson, 1979, 1985) and are characterized by large CEC numbers (Serra, 1984; Ellis, 1987). A standard technique to measure the CEC of rocks (Kejdahl method) is described by Ridge (1983). A cation not native to the rock is fixed on the exchangeable clay sites. The fixed cations are then deliberately removed and their quantity measured.

Each of the 65 samples was crushed, and a 1–2-g quantity was selected after thorough mixing. The samples were made water-wet to disperse the clays, and then washed and centrifuged three times with ammonium acetate in order to locate an ammonium ion at each of the potential exchangeable clay sites. Once diluted with water and ethyl alcohol, sodium hydroxide was used to replace the ammonium ions. Finally, the ammonium ions were condensed in a reducing environment, collected as ammonia, and titrated in the Kejdahl unit with hydrochloric acid. Labo-

Table 1. Petrologic description and values of resistivity, CEC, and porosity of samples from Hole 504B.

Unit	Piece no.	Description	Alteration	Lithology	Depth		Resistivity (ohm-m)	CEC (meq/100 g)	Porosity
					(mbrf)	(mbsf)			
2C	451	Many fractures	Phillipsite, celadonite	Pillow	3782.0	308.0	58.6	11.2	0.030
2C	466	Many fractures	Smectite (saponite), aragonite	Pillow	3783.0	309.0		15.2	
2D	514	Few cracks	Smectite (saponite), red halos	Massive flow	3789.0	315.0	111.1	10.2	0.022
2D	527	No fractures	Smectite (saponite), red halos	Massive flow	3791.0	317.0	129.5	5.1	0.018
2D	533	No fractures	Smectite (saponite), red halos	Massive flow	3792.5	318.5		6.5	
2D	563	No fractures	Smectite (saponite), red halos	Massive flow	3795.5	321.5	125.2	4.4	0.011
3A	577	One fracture	Smectite, red halos, mixed layers	Pillow	3801.0	327.0	76.8	9.4	0.034
3A	768	No fractures	Smectite, red halos, mixed layers	Pillow	3835.5	361.5		5.6	
3A	791	One fracture	Smectite, red halos, mixed layers	Pillow	3836.5	362.5		14.3	
3A	801	One fracture	Smectite, red halos, mixed layers	Pillow	3840.0	366.0	63.5	7.0	0.021
9	1180	Breccia	Intense smectite alteration, red halos	Breccia	3897.5	423.5		39.5	
9	1183	No fractures	Intense smectite alteration, red halos	Massive unit	3898.0	424.0	32.8		0.037
9	1192	A small crack	Intense smectite alteration, red halos	Massive unit	3899.0	425.0	50.9	13.3	0.034
10	1210	A small crack	Intense smectite alteration, red halos	Massive unit	3901.0	427.0	98.9	9.0	0.022
10	1213	No fractures	Intense smectite alteration, red halos	Massive unit	3901.5	427.5	132.0	9.3	0.019
14	1254	No fractures	Smectite (saponite), red halos	Massive unit	3906.5	432.5		10.1	
16	1365	Small cracks	Smectite (saponite), red halos	Pillow	3918.0	444.0	170.8	6.3	0.015
24	300	One fracture	Smectite (saponite), Na zeolite	Massive flow	4017.0	543.0		8.3	0.025
24	315	A small crack	Smectite (saponite), Na zeolite	Massive flow	4019.0	545.0	79.2	6.4	0.025
24	324	No fractures	Smectite (saponite), Na zeolite	Massive flow	4021.0	547.0		6.1	
25	342	Few fractures	Smectite, Na zeolites, red halos, calcite	Pillows	4024.0	550.0		14.0	
25	359	Cracks	Smectite, Na zeolites, red halos, calcite	Pillows	4026.0	552.0		7.5	
25	383	Cracks	Smectite, Na zeolites, red halos, calcite	Pillows	4028.0	554.0		7.1	
25	392	Few fractures	Smectite, Na zeolites, red halos, calcite	Pillows	4029.5	555.5		13.0	
27	501	No fractures	Na zeolites, smectite (saponite), talc	Massive flow	4050.5	576.5	210.6	6.1	0.013
27	538	No fractures	Minor zeolites, smectite (saponite)	Massive flow	4053.5	579.5	142.9		
27	569	A small crack	Minor zeolites, smectite (saponite)	Massive flow	4055.5	581.5	188.0	7.1	0.013
27	575	No fractures	Green smectite (saponite)	Massive flow	4056.5	582.5	179.9		0.011
27	600	No fractures	Green smectite (saponite)	Massive flow	4058.5	584.5	175.2	4.7	0.011
27	622	No fractures	Green smectite (saponite)	Massive flow	4060.5	586.5	131.1		0.014
30C	836	Cracks	Green smectite (saponite)	Thin flow	4116.5	642.5		11.3	
30C	842	No fractures	Smectite (saponite), pyrite	Thin flow	4118.0	644.0	124.7	6.7	0.014
30C	855	A fracture; cracks	Smectite (saponite), pyrite	Thin flow	4120.0	646.0	77.6	8.4	0.017
34	985	No fractures	Smectite (saponite), pyrite	Massive flow	4142.0	668.0	201.2	5.2	0.012
34	998	One crack	Smectite (saponite), pyrite	Massive flow	4143.5	669.5	73.1	8.9	0.019
34	1013	No fractures	Smectite (saponite), pyrite	Massive flow	4150.0	676.0	103.8	5.0	0.018
34	1019	Two large cracks	Smectite (saponite), pyrite	Massive flow	4152.0	678.0	94.8	5.5	
34	1024	Few cracks	Smectite (saponite), talc	Massive flow	4154.5	680.5	113.8	5.0	0.015
34	1033	No fractures	Smectite (saponite), talc	Massive flow	4155.5	681.5		6.3	
34	1041	One fracture	Smectite (saponite), talc	Massive flow	4157.0	683.0	136.6	5.7	0.018
45	1497	Many fractures	Smectite (saponite), quartz	Pillow	4261.0	878.0	89.5	5.9	0.028
45	1502	No fractures	Smectite (saponite), quartz	Pillow	4261.5	877.5		5.8	
49	1564	No fractures	Smectite (saponite), pyrite	Massive unit	4302.0	828.0		7.0	
50	1AA	Many fractures	Anhydrite, mixed-layer clays	Pillow	4319.5	845.5		9.2	
51	7C	Many fractures	Anhydrite, mixed-layer clays	Dike	4321.0	847.0	67.8	11.1	0.023
51	11B	No fractures	Anhydrite, mixed-layer clays	Dike	4323.0	849.0	108.5	7.8	0.016
59	3D	One fracture	Anhydrite, mixed-layer clays	Thin flow/dike	4374.0	900.0	86.4	1.1	0.037
59	3F	Breccia	Anhydrite, mixed-layer clays	Breccia	4374.5	900.5		2.3	
63	1	Breccia	Chlorite, laumontite, pyrite, talc, quartz	Breccia	4384.5	910.5	19.9	12.2	0.132
63	1A	Breccia	Chlorite, laumontite, pyrite, talc, quartz	Breccia	4385.0	911.0	63.6	7.6	0.042
63	10AA	Breccia	Chlorite, laumontite, pyrite, talc, quartz	Breccia	4386.0	912.0		16.1	
63	12AA	Breccia	Chlorite, laumontite, pyrite, talc, quartz	Breccia	4386.5	912.5		2.2	
73	4C	No fractures	Chlorite, laumontite, quartz, pyrite, ...	Massive unit	4462.5	988.5	85.3	6.2	0.033
73	6	Two fractures	Chlorite, laumontite, quartz, pyrite, ...	Breccia	4465.0	992.0	36.6	25.4	0.102
74	21AA	Many fractures	Chlorite, laumontite, calcite, pyrite, ...	Massive unit	4466.0	993.0		1.8	
74	10B	One fracture; many cracks	Chlorite, laumontite, calcite, pyrite, ...	Massive unit	4468.5	994.5	295.3	9.6	0.015
74	22A	Breccia	Chlorite, laumontite, calcite, pyrite, ...	Massive unit	4469.5	995.5		11.1	
90	36AA	One fracture	Chlorite, laumontite, pyrite, mixed-layer clays	Massive unit	4515.0	1041.0		7.1	
106	42AA	No fractures	Chlorite, laumontite, pyrite, mixed-layer clays	Massive unit	4575.5	1101.5		5.2	
109	44AA	Cracks	Chlorite, laumontite, mixed layer clays, ...	Massive unit	4593.0	1119.0		3.0	
118	48AA	No fractures	Smectite (saponite), pyrite, talc, ...	Massive unit	4648.0	1174.0		3.2	
129	60AA	No fractures	Smectite, pyrite, talc, mixed-layer clays, ...	Massive unit	4711.0	1237.0		3.9	
139	68A	No fractures	Smectite, pyrite, talc, mixed-layer clays, ...	Massive unit	4761.0	1287.0		2.3	
141	71AA	No fractures	Smectite, quartz, talc, mixed-layer clays, ...	Massive unit	4779.0	1305.0		1.7	
148	80AA	One fracture	Chlorite, laumontite, anhydrite, talc, ...	Massive unit	4815.0	1341.0		3.2	

ratory tests on standards indicate that this technique has a precision of 0.1 meq/100 g and a sensitivity of the order of 0.5 meq/100 g. The results are expressed in milliequivalents per 100 g of rock or in milliequivalents per liter, if converted into a CEC per unit pore volume (referred to as  $Q_v$ ).

#### Porosity and Electrical Resistivity Measurements

Porosity and electrical resistivity were measured on the 36 minicores of basalt, each 25 mm in diameter and 13 to 23 mm long. The samples

were cut from the working halves of the recovered cores (lithology described in detail in Adamson, 1985; Becker, Sakai, et al., 1988). Each minicore was cut perpendicular to the axis of the original core, and the measurements of electrical resistivity were made along the axis of these minicores. These measurements are therefore primarily representative of the "horizontal" resistivity of the bulk rock.

The porosity was determined by standard immersion methods. The core plugs were saturated with distilled water in an evacuation cell for 48 hr. For determination of dry weight, the plugs were dried at 65°C for

12 hr. Because the instrument precision is  $\pm 0.0001$  g and the reproducibility  $\pm 0.0005$  g, an experimental error of about 0.001 (0.1%) is inherent to this technique for porosity measurements. The electrical resistivity of the 36 samples was measured at 23.5°C and atmospheric pressure after they were flushed with distilled water, dried, and then saturated with a 0.195-ohm-m NaCl solution (29,000 ppm). A 10 mV, 50 Hz signal was applied to the samples with a Wayne-Kerr bridge to make measurements at a frequency similar to those used *in situ* by the dual laterolog. The resistivity was measured by attaching stainless-steel electrodes to both ends of each core plug, and a teflon wrap was applied to the cylinder surfaces in order to prevent desaturation during the course of the measurements. Although the instrumental error on the resistivity measurement is on the order of 1%, the overall error was as high as 5%, because of the difficulty in achieving a reproducible contact between the samples and the steel electrodes.

**RESULTS**

The results of the physical and chemical measurements on Hole 504B samples are summarized in Table 1 for the 65 analyzed samples. The average values of each measured physical property are given in Table 2 with respect to (1) lithologic type and (2) large-scale layers of the basement.

**Cation Exchange Capacity**

A clear zonation of the results is observed according to depth and, consequently, alteration facies of the recovered rocks (Fig.

1). This zonation is comparable to that observed in cores, thin sections, and geochemical logs (Alt et al., 1985, 1986; Anderson et al., this volume; Table 1). The quasiuniform presence of saponites (an Fe-rich trioctahedral smectite) formed due to the alteration of olivine is reflected by high values of CEC in the extrusive part of the crust. In the massive flows of Layers 2A and 2B, the average CEC is high (5.8 meq/100 g, with a standard deviation of 1.2 meq/100 g; Table 3), even though a small amount of alteration should be expected from (1) the low average porosity (1.4%; SD = 0.3%; Table 2) and (2) the absence of fractures in most of the analyzed samples. The fracture-free samples (Fig. 1) typically have the lowest CEC values in this part of the crust. In the more porous and fractured pillows (Fig. 1), the average CEC value increases to 10.2 meq/100 g (and a larger standard deviation with 6.3 meq/100 g), probably in relation to the randomness of the samples with regard to the fracturing process and the associated alteration mineral distribution. In the massive units of Layer 2C, where greenschist facies alteration is observed, the average CEC value decreases to 4.3 meq/100 g, with a small standard deviation (Table 2). This change in alteration facies was observed at about 895 mbsf, or 4370 m below rig floor (mbrf), in cores and thin sections (Emmermann, 1985; Alt et al., 1985, 1986). With respect to the lower temperature facies of alteration, greenschist facies are characterized in Hole 504B by fewer smectites, an increasing amount of chlorite, and nu-

**Table 2. Average physical properties of lithologic types and large-scale layers of the oceanic crust.**

	Lithology	Porosity (%)	Resistivity (ohm-m)	CEC (meq/100 g)
Hole 504B		2.7 (SD = 2.1)	116.1 (SD = 69.2)	8.1 (SD = 5.8)
Layers 2A and 2B	Pillows	2.3 (SD = 0.7)	89.5 (SD = 35.6)	10.2 (SD = 6.3)
Layers 2A and 2B	Flows	1.4 (SD = 0.3)	146.1 (SD = 48.4)	5.8 (SD = 1.2)
Layer 2C	Breccias	8.7 (SD = 5.9)	39.9 (SD = 21.9)	4.3 (SD = 2.5)
Layer 2C	Massive units	2.8 (SD = 0.8)	155.7 (SD = 60.7)	9.8 (SD = 5.3)
East Pacific Rise (13°N)	Pillow			1.1 (SD = 0.2)

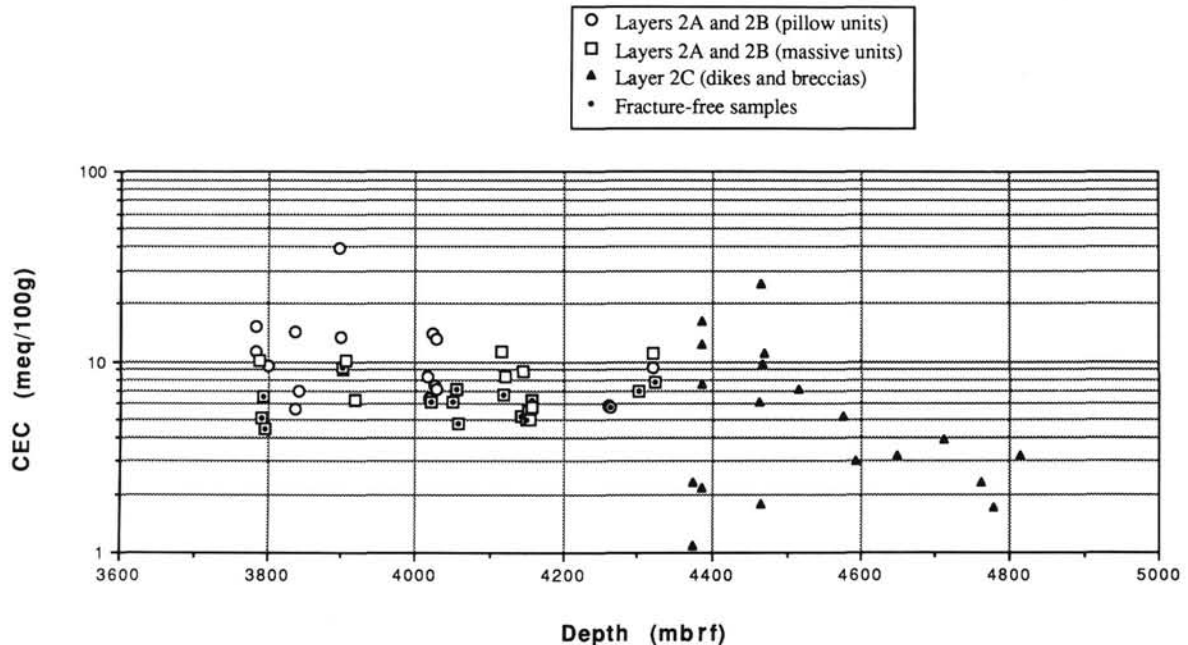


Figure 1. Laboratory measurements of CEC plotted as a function of depth in Hole 504B. The decrease in the amount of smectite (mostly saponites) from the upper part of the basement (Layers 2A and 2B) to the sheeted dikes of Layer 2C (characterized by greenschist facies of alteration) is reflected in a discernible decrease of CEC within Layer 2C. The fracture-free samples of Layers 2A and 2B commonly have the lowest CEC values.

**Table 3. Summary of the parameters of Archie's law in crystalline rocks ( $a \neq 1.0$ ).**

Context	Hole	Location	Age (Ma)	Rock type	$a$	$m$	Source
Oceanic	396B	Mid-Atlantic Ridge	13	Basalt	12.50	1.33	Core/log
			109	Basalt	11.40	1.20	Core
	417D	Bermuda Rise		Basalt	26.40	0.88	Log
				Basalt (fresh)	29.50	1.16	Log
				Basalt (altered)	11.50	1.85	Log
	504B	Costa Rica Rift	5.9	Basalt	9.10	1.05	Core
				Basalt (massive flows only)	22.00	1.06	Log
Continental	Falkenberg	Oberpfalz, FRG	—	Granite	4.10	1.08	Core

merous poorly conductive minerals such as talc, quartz, calcite, epidote, actinolite, laumontite, anhydrite, and sphene. The intense alteration of brecciated regions within the dikes of Layer 2C is, however, reflected by a high average CEC (9.8 meq/100 g) and characterized by a large variability (SD = 5.3 meq/100 g). Such variability reflects the significant segmentation of the lower crust in terms of fluid circulation, even though the widespread alteration into greenschists indicates a fairly uniform regime of hydrothermal metamorphism. This lack of lateral hydraulic connectivity between dikes might be the reason why the lowest value of CEC was measured in samples recovered at about 900.0 mbsf, in the transition zone, near extremely altered samples.

For example, sample 3D of Unit 59 (Table 1; a dike or a thin flow?) gave by far the lowest value of the entire column, 1.1 meq/100 g (Figs. 1 and 3). As part of the four repeatability checks of these CEC measurements, another sample of a few grams selected from 59-3D was measured as 1.4 meq/100 g. This repeatability was considered excellent, considering the variability of the degree of alteration from one sample to another. The three other samples similarly retested (25-383, 25-392, and 73-6) gave somewhat less compatible results (a repeatability under 15%), with a variability of 1.0 meq/100 g for each sample of Unit 25 (pillows) and 1.7 meq/100 g for the breccia of Unit 74 (otherwise one of the highest CEC values measured—25.4 meq/100 g). The low values of CEC measured on sample 59-3D are comparable to those measured on three samples from fresh pillows dredged on the East Pacific Rise at 13°N, on zero-age crust (Table 3); therefore, these low CEC values are characteristic of a small amount of alteration. Another possible explanation for these low values might arise if Unit 59 is an off-axis intrusive unit (dike or sill), which would be less exposed than other units to intense near-axis alteration.

In conclusion, the CEC measurements on Hole 504B samples are characterized by higher values in the fractured pillows and breccias than in the massive units and by an overall decrease of conductive-clay content with increasing depth, which can be related to the decrease in the amount of smectites with increasing depth (Emmermann, 1985; Alt and Emmermann, 1985; Alt et al., 1985, 1986). In the following, the relation of CEC to resistivity and porosity is studied.

### Porosity and Electrical Resistivity

From the 36 minicores sampled, only 33 pairs of measurements were successful, because three of the minicores split along fracture planes during the trimming of parallel faces for resistivity measurements. The apparent formation factor, defined as the resistivity of the rock divided by the resistivity of the fluid ( $FF = R_o/R_w$ ), is given in Table 1 and summarized in Figure 2. The terminology "apparent formation factor" is used because  $FF$  was derived from a single fluid resistivity (at  $R_w = 0.195$  ohm-m), an approximation for seawater at about 24.0°C. The results were summarized for each lithologic type, with average values computed for porosity and resistivity (Table 2). The fracture-free samples from the massive flows of Layers 2A and 2B (Fig.

2) are more resistive and less porous than the fractured ones and those from the more altered pillows (Fig. 2), as observed in previous studies (Karato, 1983, 1985; Christensen and Salisbury, 1985; Hyndman and Drury, 1976). The samples from Layer 2C (Fig. 2) generally exhibit larger resistivities than the samples from Layers 2A or 2B for a given porosity, even though most of them are fractured or brecciated (Tables 1 and 2). Even higher values of resistivity should consequently be expected from the massive units of Layer 2C, as verified *in situ* with values as high as 2000 ohm-m (Pezard and Anderson, this volume). Overall, the data plotted on Figure 2 can be represented by a regression law such as

$$FF = (9.1)\phi^{-1.05}.$$

In conclusion, the influence of alteration on the porosity-resistivity relationship can be represented as a progression from a region of low porosity-high apparent formation factor to one of higher porosity and lower formation factor.

In a similar fashion, an inverse correlation between apparent formation factor and CEC appears on Figure 3. The fracture-free samples, previously observed as having the lowest porosity and the highest formation factor of the data set, have here the lowest CEC. Such a correlation confirms the contribution of the alteration minerals to the conductivity of these basalts, without ruling out the possibility of electrolytic conduction in the pore spaces. To the contrary, the large variability of alteration phases observed in Layer 2C leads to a less clear relationship. The breccias (such as samples 63-1 and 73-6; Table 1) and fresh units (e.g., sample 59-3D) of Layer 2C clearly stand out of the overall trend (Fig. 3). These observations are discussed in the following in the context of previous studies of the relationship between porosity and apparent formation factor for crystalline (and particularly basaltic) rocks.

### DISCUSSION

The relation between resistivity and porosity was initially proposed by Sundberg (1932), and then experimentally derived for sedimentary rocks by Archie (1942), based on the analysis of resistivity measurements made on cores saturated with fluids of varying salinity. This "intrinsic" formation factor was consequently defined as related to porosity by the simple power law:

$$FF = \phi^{-m},$$

where  $m$  is cementation factor of the sedimentary rock and is thought to be related to the degree of cementation of individual grains. Winsauer and McCardell (1953) developed a more general law:

$$FF = a\phi^{-m},$$

where the factor  $a$  is a constant. The significance of  $a$  and  $m$  for sedimentary rocks has been much debated since (Keller and

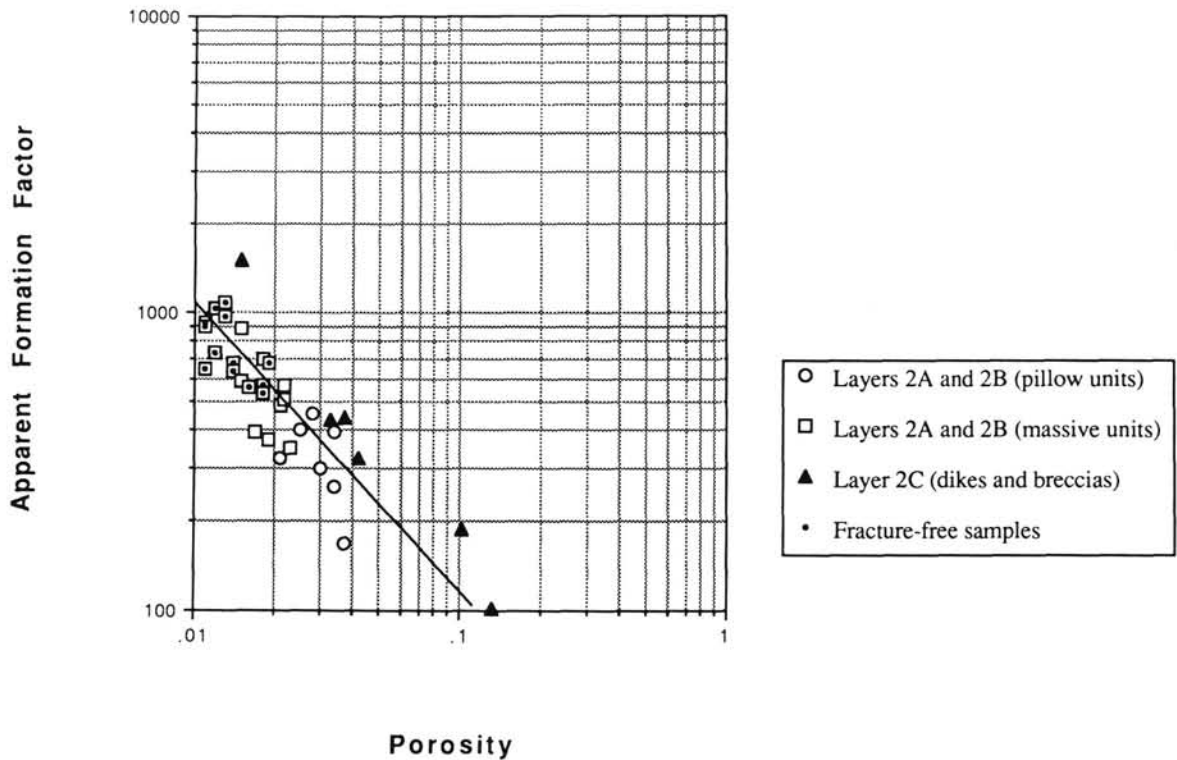


Figure 2. Apparent formation factor (determined at  $R_w = 0.195$  ohm-m) plotted vs. porosity for 33 samples of basalt from Hole 504B. An inverse relationship is observed, with the samples from the sheeted dikes and breccias of Layer 2C more resistive at equivalent porosity than those from Layers 2A and 2B. The fracture-free samples of Layers 2A and 2B (Table 1) have the lowest porosity and the highest apparent formation factor. The entire data set can be represented by a regression similar to Archie's law, with  $a = 9.1$  and  $m = 1.05$ .

Frischknecht, 1966; Jackson et al., 1978) and can be summarized as follows. The exponent  $m$  depends primarily on the shape of individual particles, and increases as sphericity decreases, from a value of 1.3 for glass spheres (Wyllie and Gregory, 1953) to 1.6 for a natural sand (Archie, 1942; Jackson et al., 1978) and up to 2.0 and higher for sheetlike clays (Atkins and Smith, 1961). In these rocks, the tortuosity of the intergranular pore space (with reference to particle shape and cementation of the pore space) appears to be the controlling factor of  $m$ , referred to in recent texts as the "tortuosity factor" (Jackson et al., 1978; Pape and Worthington, 1983; Serra, 1984; Lovell, 1985; Pape et al., 1985; Ellis, 1987). The factor  $a$  seems more related to the type of porosity, with values  $< 1$  for rocks with equal-shaped intergranular porosity and  $> 1$  for rocks with elongated-crack porosity.

In an interesting analogy to water-bearing sedimentary rocks, the same power law was applied to rocks containing partial melt, with much emphasis on the geometry and connectivity of the fluid phase (Waff, 1974; Shankland and Waff, 1977; Hermance, 1979). Theoretical studies of the conductivity of porous media suggested that Archie's law reflects in fact the distribution in a highly resistive matrix of connected vs. isolated pores (Shankland and Waff, 1974; Madden, 1976). In that sense, Madden (1976) showed that the resistivity of a random network of cracks and pore channels was relatively insensitive to the topology of its interconnections, and that, in low-porosity rocks, the conductivity is controlled by the microcrack population (which represents only a fraction of the total porosity). Similarly, Shankland and Waff (1974) concluded that the porosity structure is essential in the control of the electrical resistivity of composite materials, and that the measured (or observed) porosity might not be equivalent to the space that actually controls the electrical

conduction. In addition, two of their observations seem crucial to the understanding of Archie's analog for low-porosity crystalline rocks such as basalt. First, in cases where  $m$  approaches 1.0, Shankland and Waff (1974) stated that the porosity is a direct measurement of the conducting volume. Second, they argued that the absence of a critical porosity (i.e., a lower limit) emphasizes that conducting microcracks have multiple intersections. More recently, the concept of self similarity (Mandelbrot, 1977) was used in a similar way by Pape et al. (1982, 1985) with a so called pigeon-hole model aimed at providing a structural representation of microfissures in granite. In this way, a dendritic system of structures and substructures is accounted for to the finest scale.

#### Effects of Pressure on the Electrical Resistivity of Rocks

The most detailed study so far on the effects of pressures up to 10 kbar on the electrical resistivity of saturated rocks was carried out on a wide variety of rock samples by Brace et al. (1965) and Brace and Orange (1968a, 1968b). They found that porosity and resistivity can be related by the power given previously as derived by Archie (1942) for sedimentary rocks:

$$FF = \phi^{-2.0}$$

As confirmed by Drury and Hyndman (1979), Rai and Manghnani (1981), and Olhoeft (1981), the pressure dependence of resistivity is generally small beyond 100 MPa.

The fit of this empirical law over three orders of magnitude of porosity for such a diverse collection of rocks certainly expresses the general character of the relationship between porosity and resistivity (or formation factor) at high pressures. How-

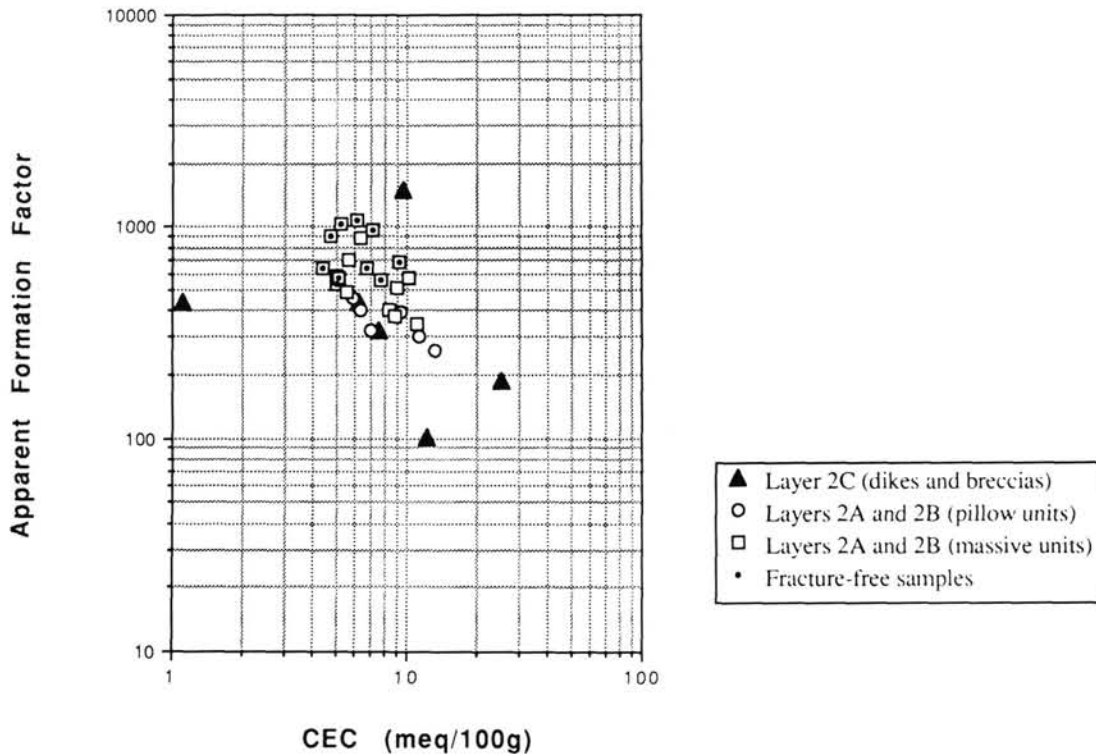


Figure 3. Apparent formation factor (determined at  $R_w = 0.195$  ohm-m) plotted vs. CEC for Hole 504B. An inverse correlation is observed in the upper part of the basement (Layers 2A and 2B), but the samples from Layer 2C do not appear to fit this trend. The fracture-free samples of Layer 2A and 2B have the highest apparent formation factor and the lowest CEC values. The largest CEC values within Layers 2A and 2B are commonly recorded in the pillow units.

ever, the comparison of a single plot of diabase, slate, sandstone, and limestone, for example, cannot be rigorously justified because of the widely differing character of their respective pore space distributions. Although it seems natural to expect a continuity between water and, for example, Neogene seafloor sediments for the law relating porosity to formation factor, it is difficult to understand why crystalline rocks, with porosities on the order of a fraction of a percent, should be compared to a fictitious rock with 100% porosity (and consequently a formation factor of one).

Many authors have shown, in fact, that porosity alone cannot be considered as the sole property controlling the resistivity of water-saturated rocks at high pressure and that  $m$  is generally observed to vary from 1.0 to 2.0, with values close to 1.0 when the conductivity is dominated by microfissure conduction (Keller and Frischknecht, 1966; Brace and Orange, 1968a; Shankland and Waff, 1974; Shankland, 1975; Madden, 1976; Jackson et al., 1978; Kirkpatrick, 1979; Serra, 1984; Pape et al., 1985; Broglia and Moos, 1988). As a consequence, it initially appears that the relation between the resistivity of rocks and the topology of cracks and pore space is a matter that should be treated separately for each individual rock.

In this respect, Brace and Orange (1968a) have shown that the resistivity of crystalline rocks subjected to increasing compressive stress drops abruptly to more than half their fracture stress. The observed decrease of  $m$  from the initial value of 2.0 to about 1.0 for the analyzed samples is due to the comparatively small change in pore volume occurring as dilatancy develops. Such a low  $m$  value might consequently be derived for rocks once subjected to intense stresses. Relict features of such stresses can be traced in microscopic investigations of structural or alteration sequences. Hydrothermal circulation, if occurring

at the same time as dilatancy, can "freeze in" the stress regime when plugging the rock microcracks with alteration products, with a low  $m$  value remaining as a signature of these once-intense deviatoric stresses.

#### Effect of Clays and Zeolites on Resistivity

The surface conduction associated with the presence of clays and zeolites was first mentioned as playing an important role in decreasing the electrical resistivity of sedimentary rocks by Winsauer and McCardell (1953) and Hill and Milburn (1956) and was then accounted for in porosity-resistivity relationships by Waxman and Smits (1968) with a modified power law such as

$$FF'' = (C_w + B \cdot Qv)/C_o,$$

where

- $FF''$  = formation factor of the altered rock,
- $C_w$  = conductivity of the pore fluid,
- $B$  = equivalent conductance of the sodium ions absorbed onto the alteration minerals' surfaces,
- $Qv$  = CEC of the rock normalized to unit volume (Serra, 1984),
- $C_o$  = conductivity of the fluid-bearing rock.

Rink and Schopper (1974) and Clavier et al. (1977) developed more sophisticated models (reviewed in Pape and Worthington, 1983; Serra, 1984; and Ellis, 1987) referring also to the analogy of resistors in parallel used by Waxman and Smits (1968) to describe the conductance of clay-bearing rocks. In order to account for the presence of clays, these authors emphasized the need to determine the intrinsic formation factor with measure-

ments made using different saturating-fluid salinities, rather than the apparent formation factor obtained from only one point (see in particular Worthington, 1985). Here again, the behavior of the rock-alteration minerals-fluid assemblage at low fluid conductivity depends considerably on the pore space distribution. For example, Clavier et al. (1977) showed that the apparent formation factor decreases to zero at low resistivity for shaly sands, whereas Pape et al. (1985) found that it rises to infinity in slightly altered granites (in fact,  $1/FF$  goes to zero) and that conduction at low fluid salinity is primarily due to the interlayer conductivity of the clays. Such opposing behaviors stress the need to consider each assemblage individually in order to access the appropriate small-scale conduction mechanism.

In the context of ocean drilling, the influence of surface conductivity on the resistivity of basalts was discussed by Olhoeft (1981), Drury and Hyndman (1979), and Karato (1985), among others. The analysis of oceanic samples has shown that the presence of alteration minerals does not modify the resistivity of low-porosity samples, with activation energies close to that of seawater. On the other hand, Olhoeft (1981) showed that surface conduction of clays, although negligible at low temperature, becomes as important as pore conduction at about 80°C and is predominant at higher temperatures. Such a temperature dependence might then play an important role in controlling the resistivity of *in-situ* measurements in deep boreholes, such as Hole 504B.

#### Formation Factor of Mid-Ocean Ridge Basalts

The nature of the porosity of crystalline rocks and basalts, in particular, was discussed at length by Brace (1971), Mathews et al. (1983), and Becker (1985) and is generally described as consisting of three types of pores:

1. Equant vesicles, mostly absent in the cores recovered from Hole 504B, and grain boundaries that might create a poorly connected path for the current.
2. Microcracks present at the scale of individual minerals are commonly defined as spaces with a characteristic length of about 100  $\mu\text{m}$  and an aspect ratio from 0.001 to 0.00001 (Simmons and Richter, 1974); as such, these microcracks are possible candidates to constitute the small-scale network required by low  $m$  values.
3. Large open cracks and voids, commonly encountered within seismic Layer 2A (Houtz and Ewing, 1976; Newmark et al., 1985; Pezard and Anderson, this volume), associated with collapse structures that originated from drained pillow lava, tubes, or flow breccias, talus, and rubble (Hekinian, 1984; Hekinian et al., 1983; Mathews et al., 1983). These large fractures are either plugged with alteration products or filled with fluid, in which case they constitute the main permeability channels in the upper part of the oceanic basement. Such porosity cannot be studied in the laboratory, stressing the need for *in-situ* experiments to obtain an accurate representation of physical properties in the upper crust.

The first two types of pore space, however, are typically found in cores analyzed in the laboratory. Porosity-formation factor relationships might vary from *in situ* to laboratory data sets because the scales of investigation are different. Consequently, care should be exerted in comparing them. Over the years, many authors have tried to relate porosity to the formation factor of mid-ocean ridge basalts (MORB), mainly with two types of regression laws, both of which are similar to Archie's empirical formula. In the first category of regressions,  $a$  is fixed to 1.0 as in Archie (1942) or Brace et al. (1965). In the second category,  $a$  is a constant commonly larger than 1.0, as suggested by Keller and Frischknecht (1966) for this type of pore space distribution.

For the models of the first kind,  $m$  was found mostly to be equal to, or greater than, 2.0 (Hyndman and Drury, 1976; Drury and Hyndman, 1979; Cann and Von Herzen, 1983; Mathews et al., 1983), with values such as 2.50 (from cores), 2.40 (from cores), 2.21 (from logs), and 2.20 (from logs), respectively. Keeping  $a$  equal to 1.0 consequently equates to forcing the regression line of Figures 2 and 4 through an imaginary point with 100% porosity (and  $FF = 1.0$ ), as mentioned previously. In addition, these studies cover a porosity range from 3.0% to 20.0%, with most of the data between 6.0% and 12.0%. For basalts from the Galapagos, Karato (1983) found  $m = 1.91$  (Sites 506, 507, 508, and 510), and  $m = 1.67$  from measurements made on cores with porosities ranging from 2.0% to 7.0% (Hole 504B; Karato, 1985). The present data set gives  $m = 1.59$  if fitted with  $a = 1.0$ . The tendency for  $m$  to increase (or steepen) with increasing porosity appears from the comparison of these results. Because the measurements made on cores have shown that large values of porosity are associated with low resistivity (Fig. 2) and important alteration (Fig. 3), the increase of  $m$  might reflect an increase in the tortuosity of the pore space, as described in previous studies (Jackson et al., 1978; Pape and Worthington, 1983; Serra, 1984; Pape et al., 1985). Therefore, such a relation does not necessarily equate to a decrease in the connectivity of the pore space (such porosity might not be "hydraulically" connected after plugging from hydrothermal activity), as commonly proposed to explain large values of  $m$ .

Choosing  $a = 1.0$  and  $m = 2.0$  in order to convert the large-scale resistivity data recorded in Hole 504B into a porosity profile, Becker (1985) noted that for a deep hole penetrating both fractured and altered pillows and relatively fresh massive units, "a single resistivity-porosity relationship cannot realistically be expected to hold throughout." This suggests that only samples compatible in terms of texture and porosity can be compared in analyzing the pore space distribution of a rock type. In consideration that Archie's equation is originally empirical, the conceptual constraint on the regression that  $FF = 1.0$  when  $\phi = 100\%$  clearly has no bearing on an empirical equation established for low porosities. In conclusion, artificially fixing  $a = 1.0$  for a wide distribution of rock types leads to erroneous conclusions.

For the more appropriate models with  $a$  other than 1.0 (e.g., Kirkpatrick, 1979; Salisbury et al., 1980; Broglia and Moos, 1988), low values of  $m$  (such as 1.33, 1.20, 1.16, and 1.06) and high values of  $a$  were generally obtained (Table 3). The initial studies based partly on the analysis of logs certainly suffered here again from erroneous evaluations of the porosity from the neutron log with, for example, some values reported as high as 50.0% in 13.0-Ma crust (Hole 396B). Such high values are either correct, but equate in this case to the porosity of a sedimentary rock and consequently do not pertain to the study of the pore space of fresh basalt, or are simply overestimated. As of the date of this work, the correction of neutron logs in basalt has not been fully worked out and is still being investigated (Broglia and Ellis, 1988). The tendency to overestimate the amount of porosity consequently induces a decrease in  $m$  that makes it difficult to use in comparative studies. As a consequence, the results from Salisbury et al. (1980) are difficult to evaluate; however, a low  $m$  value of 1.20 is reported in the low range of porosity for the laboratory data (Table 3). Kirkpatrick (1979) similarly found  $m = 1.20$  for low-porosity samples from DSDP Hole 396B. The higher  $m$  value (1.80) reported for the log data in Hole 396B is also subject to the previously noted accuracy of the porosity estimate from neutron logs in basalt.

In a recent study of basalts from Hole 418A (Broglia and Moos, 1988), the log response was calibrated vs. core data and then analyzed in a discriminating approach for sections of good log quality (such as those of small borehole size). In the ex-

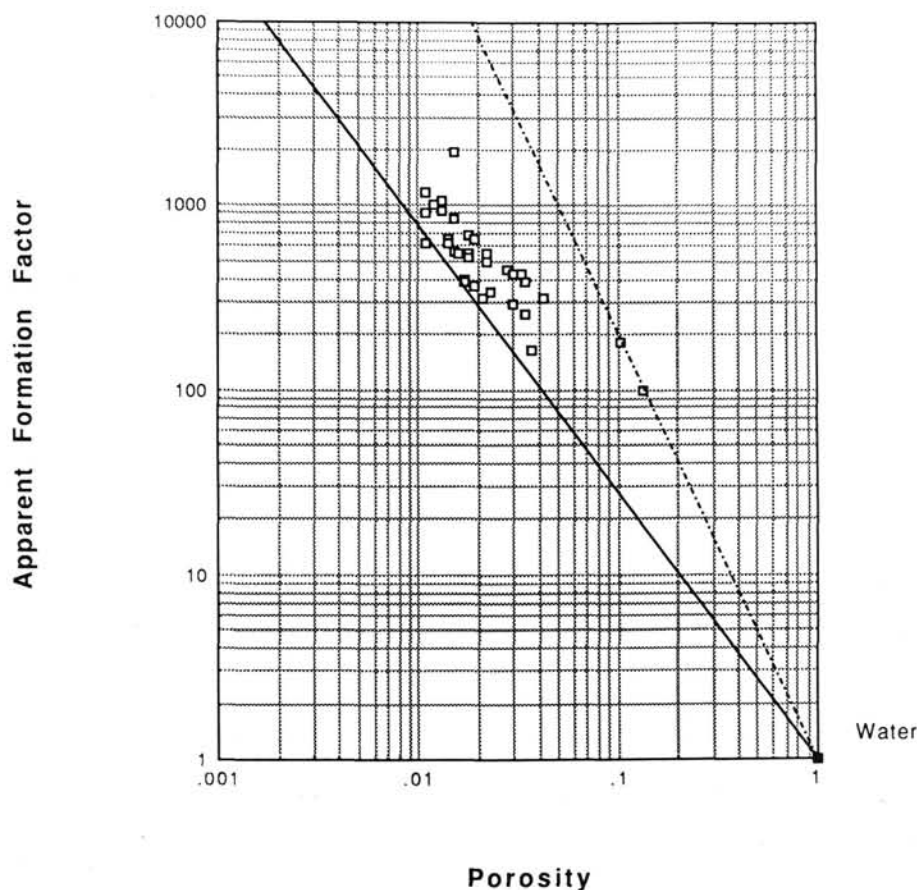


Figure 4. Same data as Figure 2 plotted over two porosity decades and including an imaginary point ( $\phi = 100\%$  and  $FF = 1.0$ ) representing water; if  $a$  is set constant and equal to 1.0.

tremely altered upper part of the basement, where the porosities (computed from neutron log data) range from 3.0% to 32.0%,  $a = 11.5$  and  $m = 1.85$ , which is similar to the log results of Kirkpatrick (1979) for Hole 396B. The lower and fresher part of the hole, where the porosities range from 2.0% to 18.0%, gave a different relation with  $a = 29.5$  and  $m = 1.16$ . The value of  $m$  is consequently larger in the altered section, which reflects an increased tortuosity of the pore space due to hydrothermal alteration. The value of 1.85 obtained in the most altered section is similar to that derived routinely for intergranular pore space (Archie, 1942; Jackson, 1978). The low  $m$  value in fresher rock contrarily indicates a pore space made mainly of microcracks. The factor  $a$  remains large in both cases and is reported to decrease with increasing alteration.

This study of young basalts from Hole 504B led to a relation with  $a = 9.1$  and  $m = 1.05$ . In comparison to the results of Broglia and Moos (1988), these values suggest that  $m$  remains low and about constant with age in fresh massive units, in this case from 5.9-Ma crust in Hole 504B to 110-Ma crust in Hole 418A. In addition, the preliminary results of the analysis of the neutron log from Hole 504B confirm that porosity and formation factor are related *in situ* by a very low  $m$  value, comparable to that found in the laboratory (Broglia and Ellis, 1988; Pezard et al., 1988; Table 3). Because the low  $m$  value found for the samples from Hole 504B refers both to massive and pillow units, the structure of the pore space of the basalt can be viewed, at the scale investigated in the laboratory, as uniform throughout the hole.

#### Changes in Pore Space Geometry of Mid-Ocean Ridge Basalts with Age

A simple model is submitted to describe the evolution of the microscopic pore space distribution of basalts that have undergone hydrothermal alteration. This model does not intend to describe the evolution of the large-scale porosity structure of the oceanic crust.

At the scale of the analyzed samples (centimeter scale), the pore space distribution of young MORB can be represented by a low  $m$  value (close to 1.0), due mainly to large aspect-ratio microfissures rather than equidimensional pores. These microcracks are rapidly filled with alteration products close to the ridge axis under intense hydrothermal circulation and at the large reactivity of basaltic rocks to water circulation. In massive units where the permeability of the rock is due solely to these microfissures, further alteration proceeds extremely slowly, if at all, as indicated by the value of  $m = 1.16$  found in 110-Ma crust (Broglia and Moos, 1988). In sections of the crust where the permeability, and therefore the circulation of fluids, is determined by the presence of large cracks or a disturbed porosity structure (such as seismic Layer 2A), the alteration of the bulk rock continues and  $m$  is observed to increase to values close to 2.0, comparable to those found for sedimentary rocks, which reflect the increasing tortuosity of the current path in the rock. Whereas the role of  $a$  is more obscure and certainly related to  $m$ , high values are obtained in all cases (Table 3) not fixed to 1.0.

Most of the alteration observed in 5.9-Ma rocks in Hole 504B (Alt et al., 1985, 1986) is constrained to occur close to the ridge axis, where the geothermal gradient is the steepest and hydrothermal circulation is the most intense. The development of near-vertical fractures and microcracks (Pezard and Anderson, this volume) is believed to have originated as a consequence of the initial cooling and quenching of the oceanic basalts (Lister, 1972; 1974), in addition to the extensional regime to which mid-ocean ridges are subjected. These cracks are sealed by intense water circulation close to the ridge axis and might evolve as the plate ages and low-temperature alteration takes over. Successive phases of reopening and growth of alteration products in these cracks were documented by Alt et al. (1985, 1986) and Emmermann (1985) for basalts from Hole 504B. The cracks consequently get wider, and probably longer with time, yielding a more tortuous current path as alteration mineral structures develop on the microscopic scale. An analytical model of such structures was described for granitic rocks by Pape et al. (1985) from a series of small-scale petrophysical analyses of the rock. Their model, based on the assumption that the pore space is chiefly constituted of microfissures, takes into account the tortuosity of both the pores and the pore surfaces on which alteration minerals develop. A power law similar to that of fresh basalt from Hole 504B was derived for these granites, with  $a = 4.1$  and  $m = 1.08$  (Table 3), which confirms the relation between a low  $m$  value and the presence of microcracks.

Such a model, based upon the repeated and widespread opening of microcracks in the rock as a result of thermal and tectonic stresses and followed by rapid plugging of these cracks through hydrothermal circulation and growth of alteration products, would explain the high CEC values measured in the massive units of Layers 2A and 2B (found as thick as 10 m). These units are otherwise observed to constitute permeability barriers to circulating fluids (Pezard and Anderson, this volume) and, therefore, to large-scale chemical fluxes within the crust. Our model consequently favors a scheme of intermittent periods of alteration for the otherwise sealed parts of the crust (Anderson et al., 1985, 1986; Becker, 1985; Becker, Sakai, et al., 1988), as opposed to the upper part (Layer 2A), which undergoes a more constant regime of alteration with permeability dominated by large-scale porosity of extrusive origin.

### CONCLUSIONS

The inverse relationship found between CEC and formation factor for samples from Layers 2A and 2B shows that the conductivity of clay and zeolites present as alteration phases of basalt cannot be ignored in deriving a porosity profile from resistivity data. The low  $m$  value obtained in relating porosity to apparent formation factor of the analyzed samples indicates that the conducting pore space of MORB is made mainly of cracks and microcracks, as observed elsewhere in thin section.

In future studies, computation from measurements made at different saturating-fluid salinities of the intrinsic formation factor of each sample is needed to derive more precise values of  $m$  and  $a$ , while accounting for the presence of clays and zeolites. In addition, the influence of temperature on clay conduction remains to be investigated in relation with CEC values in order to correct *in-situ* measurements adequately. In summation, the comparison of values of  $m$  and  $a$  obtained from different holes and based on the computation of the intrinsic formation factor in each case should lead to a more precise understanding of the evolution of the pore space of the oceanic crust with increasing age and alteration.

### ACKNOWLEDGMENTS

We would like to express our gratitude to co-chiefs Keir Becker and Hitoshi Sakai for letting us participate on ODP Leg 111. Russ Merrill

and Gerry Bode assisted us in obtaining samples from previous DSDP legs that drilled Hole 504B, and Andy Adamson kindly supplied samples studied for alteration content. We would like to thank Morton Ridge and Larry McGowan of Schlumberger Doll Research for providing their assistance with the laboratory measurements. In addition, this manuscript benefited greatly from numerous informal discussions with Jeffrey Alt, John Malpas, Daniel Bideau, Cristina Broglia, and Charlie Langmuir and thorough reviews from Roger Anderson, Paul Worthington, and Keir Becker. This work was supported by the NSF through JOI.

### REFERENCES

- Adamson, A. C., 1979. Chemistry of alteration minerals from DSDP Sites 501, 504, and 505. *In* Cann, J. R., Langseth, M. G., Honnorez, J., Von Herzen, R. P., White, S. M., et al., *Init. Repts. DSDP*, 69: Washington (U.S. Govt. Printing Office), 551-564.
- , 1985. Basement lithostratigraphy, DSDP Hole 504B. *In* Anderson, R. N., Honnorez, J., Becker, K., et al., *Init. Repts. DSDP*, 83: Washington (U.S. Govt. Printing Office), 121-127.
- Alt, J. C., and Emmermann, R., 1985. Geochemistry of hydrothermally altered basalts: DSDP Hole 504B. *In* Anderson, R. N., Honnorez, J., Becker, K., et al., *Init. Repts. DSDP*, 83: Washington (U.S. Govt. Printing Office), 249-262.
- Alt, J. C., Honnorez, J., Laverne, C., and Emmermann, R., 1986. Hydrothermal alteration of a 1-km section through the upper oceanic crust, DSDP Hole 504B: mineralogy, chemistry and evolution of seawater-basalt interactions. *J. Geophys. Res.*, 91:309-335.
- Alt, J. C., Laverne, C., and Muehlenbachs, K., 1985. Alteration of the upper oceanic crust: mineralogy and processes in DSDP Hole 504B, Leg 83. *In* Anderson, R. N., Honnorez, J., Becker, K., et al., *Init. Repts. DSDP*, 83: Washington (U.S. Govt. Print. Office), 217-248.
- Anderson, R. N., and Hobart, M. A., 1976. The relation between heat flow, sediment thickness, and age in the eastern Pacific. *J. Geophys. Res.*, 81:1968-1989.
- Anderson, R. N., Honnorez, J., Becker, K., et al., 1985. *Init. Repts. DSDP*, 83: Washington (U.S. Govt. Printing Office).
- Anderson, R. N., O'Malley, H., and Newmark, R. L., 1985. Use of geophysical logs for quantitative determination of fracturing, alteration, and lithostratigraphy in the upper oceanic crust, DSDP Holes 504B and 556. *In* Anderson, R. N., Honnorez, J., Becker, K., et al., *Init. Repts. DSDP*, 83: Washington (U.S. Govt. Printing Office), 443-478.
- Anderson, R. N., and Zoback, M. D., 1982. Permeability, underpressures, and convection in the oceanic crust near the Costa Rica Rift. *J. Geophys. Res.*, 87:2860-2868.
- Anderson, R. N., Zoback, M. D., Hickman, S. H., and Newmark, R. L., 1986. Permeability versus depth in the upper oceanic crust: *in situ* measurements in DSDP Hole 504B, eastern equatorial Pacific. *J. Geophys. Res.*, 90:3659-3669.
- Archie, G. E., 1942. The electrical resistivity log as an aid in determining some reservoir characteristics. *J. Petrol. Tech.*, 5:1-8.
- ARCYANA, 1975. Transform fault and rift valley from bathyscaph and diving saucer. *Science*, 190:108-116.
- Atkins, E. R., and Smith, G. H., 1961. The significance of particle shape in formation-factor-porosity relationships. *J. Petrol. Tech.*, 13:285-291.
- Ballard, R. D., Bryan, W. B., Heirtzler, J. R., Keller, G., Moore, J. G., and Van Andel, T. H., 1975. Manned submersible observations in the FAMOUS area: Mid-Atlantic Ridge. *Science*, 190:103-108.
- Becker, K., 1985. Large-scale electrical resistivity and bulk porosity of the oceanic crust, DSDP Hole 504B, Costa Rica Rift. *In* Anderson, R. N., Honnorez, J., Becker, K., et al., *Init. Repts. DSDP*, 83: Washington (U.S. Govt. Printing Office), 419-427.
- Becker, K., Sakai, H., et al., 1988. *Proc. ODP, Init. Repts.*, 111: College Station, TX (Ocean Drilling Program).
- Brace, W. F., 1971. Resistivity of saturated crustal rocks to 40 km based on laboratory studies. *In* Heacock, J. G. (Ed.), *The Structure and Physical Properties of the Earth's Crust*: Washington (Am. Geophys. Union), 243-255.
- Brace, W. F., and Orange, A. S., 1968a. Electrical resistivity changes in saturated rocks during fracture and frictional sliding. *J. Geophys. Res.*, 73:1433-1445.
- , 1968b. Further studies of the effect of pressure on the electrical resistivity of rocks. *J. Geophys. Res.*, 73:5407-5420.

- Brace, W. F., Orange, A. S., and Madden, T. R., 1965. The effect of pressure on the electrical resistivity of water-saturated crystalline rocks. *J. Geophys. Res.*, 70:5669-5678.
- Brogia, C., and Ellis, D. V., 1988. Response of the thermal neutron porosity log to alteration and environmental factors in basaltic rocks from ODP sites. *EOS, Trans. Am. Geophys. Union*, 69:1403.
- Brogia, C., and Moos, D., 1988. *In situ* structure and properties of 110 Ma crust from geophysical logs in DSDP Hole 418A. In Salisbury, M. H., Scott, J., et al., *Proc. ODP, Sci. Results*, 102: College Station, TX (Ocean Drilling Program), 29-47.
- Cann, J. R., and Von Herzen, R. P., 1983. Downhole logs at DSDP Sites 501, 504, and 505, near the Costa Rica Rift. In Cann, J. R., Langseth, M. G., Honnorez, J., Von Herzen, R. P., White, S. M., et al., *Init. Repts. DSDP*, 69: Washington (U.S. Govt. Printing Office), 281-300.
- Christensen, N. I., and Salisbury, M. H., 1985. Seismic velocities, densities, and porosities of Layer 2B and Layer 2C basalts from Hole 504B. In Anderson, R. N., Honnorez, J., Becker, K., et al., *Init. Repts. DSDP*, 83: Washington (U.S. Govt. Printing Office), 367-370.
- Clavier, C., Coates, G., and Dumanoir, J., 1977. The theoretical and experimental bases for the dual-water model for the interpretation of shaly sands [paper presented at the SPE 52nd Annual Fall Technical Conference, Denver, CO].
- Corliss, J. B., Dymond, J., Gordon, L. I., Edmond, J. M., Von Herzen, R. P., Ballard, R. D., Green, K., Williams, D., Bainbridge, A., Crane, K., and Van Andel, T. H., 1979. Submarine thermal springs on the Galapagos Rift. *Science*, 203:1073-1083.
- Cox, C. S., 1971. The electrical conductivity of the oceanic lithosphere. In Heacock, J. G. (Ed.), *The Structure and Physical Properties of the Earth's Crust*: Washington (Am. Geophys. Union), 227-234.
- Cox, C. S., Constable, S. C., Chave, A. D., and Webb, S. C., 1986. Controlled-source electromagnetic sounding of the oceanic lithosphere. *Nature*, 320:53-54.
- Donnelly, T., Francheteau, J., Bryan, W., Robinson, P., Flower, M., Salisbury, M., et al., 1980. *Init. Repts. DSDP*, 51, 52, 53: Washington (U.S. Govt. Printing Office).
- Drury, M. J., and Hyndman, R. D., 1979. The electrical resistivity of oceanic basalts. *J. Geophys. Res.*, 84:4537-4546.
- Edmond, J. M., Measures, C., McDuff, R. E., Chan, L. H., Collier, R., and Grant, B., 1979. Ridge crest hydrothermal activity and the balances of the major and minor elements in the ocean. *Earth Planet. Sci. Lett.*, 46:1-18.
- Ellis, D. V., 1987. *Well Logging for Earth Scientists*: New York (Elsevier).
- Emmermann, R., 1985. Basement geochemistry Hole 504B. In Anderson, R. N., Honnorez, J., Becker, K., et al., *Init. Repts. DSDP*, 83: Washington (U.S. Govt. Printing Office), 183-199.
- Francheteau, J., 1983. The oceanic crust. *Sci. Am.*, 249:114-129.
- Gass, I. G., and Smewing, J. D., 1973. Intrusion, extrusion, and metamorphism at constructive margins: evidence from the Troodos massif, Cyprus. *Nature*, 242:26-29.
- Hekinian, R., 1984. Undersea volcanoes. *Sci. Am.*, 251:46-55.
- Hekinian, R., Renard, V., and Cheminee, J. L., 1983. Hydrothermal deposits on the East Pacific Rise near 13°N: geological setting and distribution of active sulfide chimneys. In Rona, P. A. (Ed.), *Hydrothermal Processes at Sea Floor Spreading Centers*: New York (Plenum), 17-27.
- Hermance, J. F., 1979. The electrical conductivity of materials containing partial melt: a simple model from Archie's law. *Geophys. Res. Lett.*, 6:613-616.
- Hickman, S. H., Langseth, M. G., and Svitek, J. F., 1984. *In situ* permeability and pore pressure measurements near the Mid-Atlantic Ridge, DSDP Hole 395A. In Hyndman, R. D., Salisbury, M. H., et al., *Init. Repts. DSDP*, 78B: Washington (U.S. Govt. Printing Office), 699-708.
- Hill, H. J., and Milburn, J. D., 1956. Effect of clay and water salinity on the electrochemical behavior of reservoir rocks. *Trans. Am. Inst. Min.*, 207:65-72.
- Houtz, R., and Ewing, J., 1976. Upper crustal structure as a function of plate age. *J. Geophys. Res.*, 81:2490-2498.
- Hyndman, R. D., and Drury, M. J., 1976. The physical properties of oceanic basement rocks from deep drilling on the Mid-Atlantic Ridge. *J. Geophys. Res.*, 81:4042-4052.
- Hyndman, R. D., and Salisbury, M. H., 1983. The physical nature of the oceanic crust on the Mid-Atlantic Ridge, DSDP Hole 395A. In Hyndman, R. D., Salisbury, M. H., et al., *Init. Repts. DSDP*, 78B: Washington (U.S. Govt. Printing Office), 839-848.
- Jackson, P. D., Taylor Smith, D., and Stanford, P. N., 1978. Resistivity-porosity-particle shape relationships for marine sands. *Geophysics*, 43:1250-1268.
- Karato, S. I., 1983. Physical properties of basalts from the Galapagos, Leg 70. In Cann, J. R., Langseth, M. G., Honnorez, J., Von Herzen, R. P., White, S. M., et al., *Init. Repts. DSDP*, 69: Washington (U.S. Govt. Printing Office), 423-428.
- \_\_\_\_\_, 1985. Physical properties of basalts from DSDP Hole 504B, Costa Rica Rift. In Anderson, R. N., Honnorez, J., Becker, K., et al., *Init. Repts. DSDP*, 83: Washington (U.S. Govt. Printing Office), 687-695.
- Keller, G. V., and Frischknecht, F. C., 1966. *Electrical Methods in Geophysical Prospecting*: Oxford (Pergamon Press).
- Kidd, R. G. W., 1977. A model for the process of formation of the upper oceanic crust. *Geophys. J. R. Astron. Soc.*, 50:149-183.
- Kirkpatrick, R. J., 1979. The physical state of the oceanic crust: results of downhole geophysical logging in the Mid-Atlantic Ridge at 23°N. *J. Geophys. Res.*, 84:178-188.
- Lister, C. R. B., 1972. On the thermal balance of a mid-ocean ridge. *Geophys. J. R. Astron. Soc.*, 26:515-535.
- \_\_\_\_\_, 1974. On the penetration of water into hot rock. *Geophys. J. R. Astron. Soc.*, 39:465-509.
- Lovell, M. A., 1985. Thermal conductivity and permeability assessment by electrical resistivity measurements in marine sediments. *Mar. Geotechnol.*, 6:205-240.
- Luyendyk, B. P., and Macdonald, K. C., 1977. Physiography and structure of the inner floor of the FAMOUS rift valley: observations with a deep-towed instrument package. *Geol. Soc. Am. Bull.*, 88:648-663.
- Macdonald, K. C., 1983. Crustal processes at spreading centers. *Rev. Geophys. Space Phys.*, 21:1441-1454.
- Madden, T. R., 1976. Random networks and mixing laws. *Geophysics*, 41:1104-1125.
- Mandelbrot, B. B., 1977. *Fractals—Form, Chance, and Dimension*: Freeman (San Francisco).
- Mathews, M., Salisbury, M. H., and Hyndman, R. D., 1983. Basement logging on the Mid-Atlantic Ridge, DSDP Hole 395A. In Hyndman, R. D., Salisbury, M. H., et al., *Init. Repts. DSDP*, 78B: Washington (U.S. Govt. Printing Office), 717-730.
- Newmark, R. L., Anderson, R. N., Moos, D., and Zoback, M. D., 1985. Sonic and ultrasonic logging of Hole 504B and its implications for the structure, porosity, and stress regime of the upper 1 km of the oceanic crust. In Anderson, R. N., Honnorez, J., Becker, K., et al., *Init. Repts. DSDP*, 83: Washington (U.S. Govt. Printing Office), 479-510.
- Olhoeft, G. R., 1981. Electrical properties of rocks. In Touloukian, Y. S., Judd, W. R., and Roy, R. F. (Eds.), *Physical Properties of Rocks and Minerals*: New York (McGraw-Hill), 257-330.
- Pape, H., Riepe, L., and Schopper, J. R., 1982. A pigeon-hole model for relating permeability to specific surface. *Log Analyst*, 23(1):5-13 and 23(1):50 (errata).
- \_\_\_\_\_, 1985. Petrophysical detection of microfissures in granites [paper presented at SPWLA, 26th Annual Logging Symposium, Dallas, TX].
- Pape, H., and Worthington, P. F., 1983. A surface-structure model for the electrical conductivity of reservoir rocks [paper presented at the 8th European Formation Evaluation Symposium, London, U.K.].
- Pezard, P. A., Howard, J. J., and McGowan, L., 1988. Resistivity, porosity, and cation exchange capacity measurements on cores from DSDP Hole 504B. *EOS, Trans. Am. Geophys. Union*, 69:1402.
- Rai, C. S., and Manghnani, M. H., 1981. The effect of saturant salinity and pressure on the electrical resistivity of Hawaiian basalts. *Geophys. J. R. Astron. Soc.*, 65:395-405.
- Ridge, M. J., 1983. A combustion method for measuring the cation exchange capacity of clay minerals. *Log Analyst*, 24(3):6-11.
- Rink, M., and Schopper, J. R., 1974. Interface conductivity and its implications to electric logging [paper presented at SPWLA, 15th Annual Logging Symposium, Dallas, TX].
- Salisbury, M. H., Donnelly, T. W., and Francheteau, J., 1980. Geophysical logging in DSDP Hole 417D. In Donnelly, T., Francheteau, J., Bryan, W., Robinson, P., Flower, M., Salisbury, M., et al., *Init.*

- Repts. DSDP*, 51, 52, 53: Washington (U.S. Govt. Printing Office), 705-713.
- Sclater, J. G., and Francheteau, J., 1970. The implication of terrestrial heat-flow observations on current tectonic and geochemical models of the crust and upper mantle of the earth. *Geophys. J. R. Astron. Soc.*, 20:509-542.
- Serra, O., 1984. *Fundamentals of Well-Log Interpretation*: Amsterdam (Elsevier).
- Shankland, T. J., 1975. Electrical conduction in rocks and minerals: parameters for interpretation. *Phys. Earth Planet. Inter.*, 10:209-219.
- Shankland, T. J., and Waff, H. S., 1974. Conductivity in fluid-bearing rocks. *J. Geophys. Res.*, 79:4863-4868.
- \_\_\_\_\_, 1977. Partial melting and electrical conductivity anomalies in the upper mantle. *J. Geophys. Res.*, 82:5409-5417.
- Simmons, G., and Richter, D., 1974. Microcracks in rocks. In Strens, R.G.J. (Ed.), *The Physics and Chemistry of Minerals and Rocks*: London (Wiley), 105-137.
- Sleep, N. H., and Wolery, T. J., 1978. Thermal and chemical constraints on venting of hydrothermal fluids at mid-ocean ridges. *J. Geophys. Res.*, 83:5913-5922.
- Spiess, F. N., Macdonald, K. C., Atwater, T., Ballard, R. D., Carranza, A., Cordoba, D., Cox, C. S., Diaz Garcia, V. M., Francheteau, J., Guerrero, J., Hawkins, J., Haymon, R., Hessler, R., Juteau, T., Kastner, M., Larson, R., Luyendyk, B., Macdougall, J. D., Miller, S., Normark, W., Orcutt, J., and Rangin, C., 1980. East Pacific Rise: hot springs and geophysical experiments. *Science*, 207:1421-1432.
- Stern, C., and Elthon, D., 1979. Vertical variations in the effects of hydrothermal metamorphism in Chilean ophiolites: their implications for ocean floor metamorphism. *Tectonophysics*, 55:179-213.
- Sundberg, K., 1932. Effect of impregnating waters on electrical conductivity of soils and rocks. *Trans. Am. Inst. Min., Metall. Pet. Eng.*, 79:367-391.
- Waff, H. S., 1974. Theoretical considerations of electrical conductivity in a partially molten mantle and implications for geothermometry. *J. Geophys. Res.*, 79:4003-4010.
- Waxman, M. H., and Smits, L.J.M., 1968. Electrical conductivities in oil-bearing shaly sands. *Soc. Pet. Eng. J.*, 8:107-122.
- Williams, D. L., Von Herzen, R. P., Sclater, J. G., and Anderson, R. N., 1974. The Galapagos spreading centre: lithospheric cooling and hydrothermal circulation. *Geophys. J. R. Astron. Soc.*, 38:587-608.
- Winsauer, W. O., and McCardell, W. M., 1953. Ionic double-layer conductivity in reservoir rocks. *Petrol. Trans. AIME*, 198:129-134.
- Worthington, P., 1985. The evolution of shaly-sand concepts in reservoir evaluation. *Log Analyst*, 26(1):23-40.
- Wyllie, R. J., and Gregory, A. R., 1953. Formation factors of unconsolidated porous media: influence of particle shape and effects of cementation. *Petrol. Trans. AIME*, 198:103-110.
- Wyllie, R. J., Gregory, A. R., and Gardner, G.H.F., 1958. An experimental investigation of factors affecting elastic wave velocities in porous media. *Geophysics*, 23:459-469.
- Young, P. D., and Cox, C. S., 1981. Electromagnetic active source sounding near the East Pacific Rise. *Geophys. Res. Lett.*, 8:1043-1046.

**Date of initial receipt: 27 July 1988**  
**Date of acceptance: 23 February 1989**  
**Ms 111B-136**